

SEARCH FOR CRITICAL PHENOMENA IN PB+PB COLLISIONS

MIKHAIL L. KOPYTINE* FOR THE NA44 COLLABORATION

Department of Physics and Astronomy, SUNY at Stony Brook,

E-mail: Mikhail.Kopytine@sunysb.edu

I.BEARDEN^A, H.BØGGILD^A, J.BOISSEVAIN^B, L.CONIN^D, J.DODD^C,
 B.ERAZMUS^D, S.ESUMI^E, C.W.FABJAN^F, D.FERENC^G, D.E.FIELDS^B,
 A.FRANZ^F, J.J.GAARDHØJE^A, A.G.HANSEN^A, O.HANSEN^A, D.HARDTKE^I,
 H. VAN HECKE^B, E.B.HOLZER^F, T.J.HUMANIC^I, P.HUMMEL^F,
 B.V.JACAK^J, R.JAYANTI^I, K.KAIMI^E, M.KANETA^E, T.KOHAMA^E,
 M.L.KOPYTINE^J, M.LELTCHOUK^C, A.LJUBICIC, JR^G, B. LÖRSTAD^K,
 N.MAEDA^E, L.MARTIN^D, A.MEDVEDEV^C, M.MURRAY^H, H.OHNISHI^E,
 G.PAIC^F, S.U.PANDEY^I, F.PIUZ^F, J.PLUTA^D, V.POLYCHRONAKOS^L,
 M.POTEKHIN^C, G.POULARD^F, D.REICHHOLD^I, A.SAKAGUCHI^E,
 J.SCHMIDT-SØRENSEN^K, J.SIMON-GILLO^B, W.SONDHEIM^B,
 T.SUGITATE^E, J.P.SULLIVAN^B, Y.SUMI^E, W.J.WILLIS^C, K.L.WOLF^H,
 N.XU^B, D.S.ZACHARY^I.

^A Niels Bohr Institute, Denmark; ^B LANL, USA; ^C Columbia U., USA; ^D Nuclear Physics Laboratory of Nantes, France; ^E Hiroshima U., Japan; ^F CERN; ^G Rudjer Bosovic Institute, Croatia; ^H Texas A&M U., USA; ^I The Ohio State U., USA; ^J SUNY at Stony Brook, USA; ^K U. of Lund, Sweden; ^L BNL, USA.

NA44 uses a 512 channel Si pad array covering $1.5 < \eta < 3.3$ to study charged hadron production in Pb+Pb collisions at the CERN SPS. We apply a multiresolution analysis, based on a Discrete Wavelet Transformation, to probe the texture of particle distributions event-by-event, by simultaneous localization of features in space and scale. Scanning a broad range of multiplicities, we look for a possible critical behaviour in the power spectra of local density fluctuations. The data are compared with detailed simulations of detector response, using heavy ion event generators, and with a reference sample created via event mixing.

An ultrarelativistic collision of heavy ions presents a phenomenon whose most interesting features are conditioned by the large multitude of degrees of freedom involved, and yet offer an opportunity for the fundamental physics of the strong interaction to manifest itself. The very notion of a phase transition in such collisions is inherently of a multiparticle nature. Truly multiparticle observables, defined on event-by-event basis – a few have been constructed so

* ON AN UNPAID LEAVE FROM P.N.LEBEDEV PHYSICAL INSTITUTE, RUSSIAN ACADEMY OF SCIENCES

far – therefore attract attention. Recently published event-by-event analyses of the 158 GeV/A $Pb + Pb$ data either deal with a small number of events¹ or analyse properties of a large ensemble of events using a single observable (p_T) to compare different ensemble averages². In the first case, accumulation of feature information from large data sets remains open. In the second case², one can not establish a scale independency in event textures by observing a logical consequence thereof³. Furthermore, an ensemble average on a set of *post-freeze-out* events is not representative of the *pre-freeze-out* history of those events, due to the dramatic non-stationarity of the open system, with a consequent lack of ergodicity.

Here we concentrate on *texture*, or *local fluctuation* observables, where a single event determines its own correlation/fluctuation content, and the scale composition thereof manifests itself in the observables in a positive way. The idea to look at particle distributions in rapidity y to search for critical behaviour was proposed^{4,5} based upon a Ginzburg-Landau type of multihadron production theory⁴, where a random hadronic field $\phi(y)$ plays the role of an order parameter in a hadronization transition. Enhanced large scale correlations of hadrons in y at the phase transition would signal critical fluctuations in the order parameter. Stephanov and coworkers⁶ indicated a second order QCD phase transition point which should exist under certain initial conditions, within the reach of today's experiments.

In our work, a power spectrum analysis of event texture in pseudorapidity η and azimuthal angle ζ , based on a Discrete Wavelet Transformation (DWT)⁷, is performed on a number of large event ensembles sampled according to their multiplicity, thereby studying the impact parameter dependence of the observables. DWT quantifies contributions of different ζ and η scales into the overall event's texture, thus testing the possible large scale enhancement.

The SPS beam was collimated to a 1×2 mm profile. The NA44 Si pad array, installed 10 cm downstream from the target, in the magnetic field of the first dipole⁸, measured ionization energy loss of charged particles in its 512 $300 \mu\text{m}$ thick Si pads. The silicon detector had inner radius 7.2 mm and outer radius 43 mm. The detector was split *radially* into 16 rings of equal η coverage. Each ring was divided *azimuthally* into 32 sectors of equal angular coverage to form pads. The pads were read out by AMPLEX⁹ chips, one chip per sector. δ -electrons, produced by the Pb beam traversing the target, were swept away to one side by the dipole magnetic field (≤ 1.6 Tl). Only the δ -electron-free side was used in this analysis. Channel pedestals had, on the average, $FWHM = 0.48 < dE >$ of 1 MIP. In the texture analysis, every event was represented by a 2D array of the calibrated digitized amplitudes of the channels (an *amplitude array*). Empty target runs were used to measure

the background. Cross-talk in the detector was evaluated off-line.

DWT formalizes the images of the $PbPb$ collision events in pseudorapidity η and azimuthal angle ζ by expanding them into a set of functions orthogonal with respect to scale and position, and allows one to accumulate the texture information by averaging the power spectra of many events. The simplest DWT basis is the Haar one, built upon the scaling function $\phi(x) = 1$ for $0 \leq x < 1$ and 0 otherwise. If the interaction vertex lies on the detector's symmetry axis, every pad's acceptance is a rectangle in the (ζ, η) space. Then, the Haar basis is the natural one, as its scaling function in two dimensions (2D) $\Phi(\zeta, \eta) = \phi(\zeta)\phi(\eta)$ is just a pad's acceptance (modulo units). We set up a 2D wavelet basis:

$$\Psi_{m,i,j}^\lambda(\zeta, \eta) = 2^m \Psi^\lambda(2^m \zeta - i, 2^m \eta - j) \quad (1)$$

$\Phi_{m,i,j}(\zeta, \eta)$ is constructed from $\Phi(\zeta, \eta)$ similarly. Here, m is an integer scale fineness index; i and j index the discrete positions of pad centers in ζ and η ($1 \leq m \leq 4$ and $1 \leq i, j \leq 16$ because we use $16 = 2^4$ rings and 16 sectors). Different values of λ (denoted as ζ , η , and $\zeta\eta$) distinguish, respectively, functions with azimuthal, pseudorapidity, and diagonal texture sensitivity:

$$\Psi^\zeta = \psi(\zeta)\phi(\eta), \quad \Psi^\eta = \phi(\zeta)\psi(\eta), \quad \Psi^{\zeta\eta} = \psi(\zeta)\psi(\eta) \quad (2)$$

In the Haar basis, for any variable x

$$\psi(x) = \left\{ +1 \text{ for } 0 \leq x < \frac{1}{2}; -1 \text{ for } \frac{1}{2} \leq x < 1; 0 \text{ otherwise} \right\} \quad (3)$$

is the wavelet function. Then, $\Psi_{m,i,j}^\lambda$ with integer m , i , and j are known⁷ to form an orthonormal basis in $L^2(\mathbb{R}^2)$. We adopt the existing¹⁰ 1D DWT power spectrum analysis technique and expand it to 2D. Track density in an individual event is $\rho(\zeta, \eta)$ and its *local* fluctuation in a given event is $\sigma^2 \equiv \langle \rho - \bar{\rho}, \rho - \bar{\rho} \rangle$, where $\bar{\rho}$ is the average ρ in the given event. Using completeness of the basis, we expand

$$\rho - \bar{\rho} = \langle \rho, \Psi_{m,i,j}^\lambda \rangle \Psi_{m,i,j}^\lambda - \langle \bar{\rho}, \Psi_{m,i,j}^\lambda \rangle \Psi_{m,i,j}^\lambda \quad (4)$$

Notice that $\bar{\rho}$, being constant within detector's rectangular acceptance, is orthogonal to any $\Psi_{m,i,j}^\lambda$ with $m \geq 1$. Due to the orthonormality condition $\langle \Psi_{m,i,j}^\lambda, \Psi_{m',i',j'}^{\lambda'} \rangle = \delta_{\lambda,\lambda'} \delta_{m,m'} \delta_{i,i'} \delta_{j,j'}$, the $\rho - \bar{\rho}$ components for different scales do not form cross-terms in the σ^2 sum, and the sum contains no cross-terms between ρ and $\bar{\rho}$ for the four observable scales. Instead of a $\langle \rho, \Phi_{m=5,i,j} \rangle$ set, the amplitude array – its closest experimentally achievable approximation – is used as the DWT input.

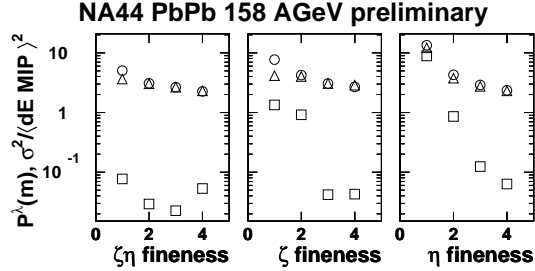


Figure 1. Power spectra of 7×10^3 events in the multiplicity bin $379 < dN/d\eta < 463$. \circ – true events, \triangle – mixed events, \square – the average event.

The Fourier images of 1D wavelet functions occupy a set of wave numbers whose characteristic broadness grows with scale fineness m as 2^m ; 2^{2m} should be used in the 2D case. In 2D, we find it most informative to present the three modes of a power spectrum with different directions of sensitivity $P^{\zeta\eta}(m)$, $P^\zeta(m)$, $P^\eta(m)$ separately. We define *power spectrum* as

$$P^\lambda(m) = \frac{1}{2^{2m}} \sum_{i,j} \langle \rho, \Psi_{m,i,j}^\lambda \rangle^2, \quad (5)$$

where the denominator gives the meaning of spectral *density* to the observable. So defined, the $P(m)$ of a random white noise field (for example) is independent of m ¹¹. In the first approximation, the white noise example provides a base-line case for comparisons in search for non-trivial effects.

We used WAILI¹² software library to obtain the wavelet expansions. Figure 1 shows the power spectra for one multiplicity range. The first striking feature is that the power spectra of physical events are indeed enhanced on the coarse scale. The task of the analysis is to quantify and, as much as possible, eliminate “trivial” and experiment-specific reasons for this enhancement.

The average event, formed by summing amplitude arrays of the measured events within a multiplicity range, and dividing by the number of events, has a much reduced texture as fluctuations cancel. However it retains the texture associated with the $d^2N/d\eta d\zeta$, with the dead channels and the finiteness of the beam’s geometrical cross-section. A better way to get rid of the “trivial” texture is to use mixed events. The event mixing is done by taking different channels from different events. Therefore, the mixed events preserve the texture associated with the detector position offset, the inherent $dN/d\eta$ shape and the dead channels. In order to reproduce the electronics cross-talk effects in the mixed event sample, mixing is done sector-wise, i.e. the sectors

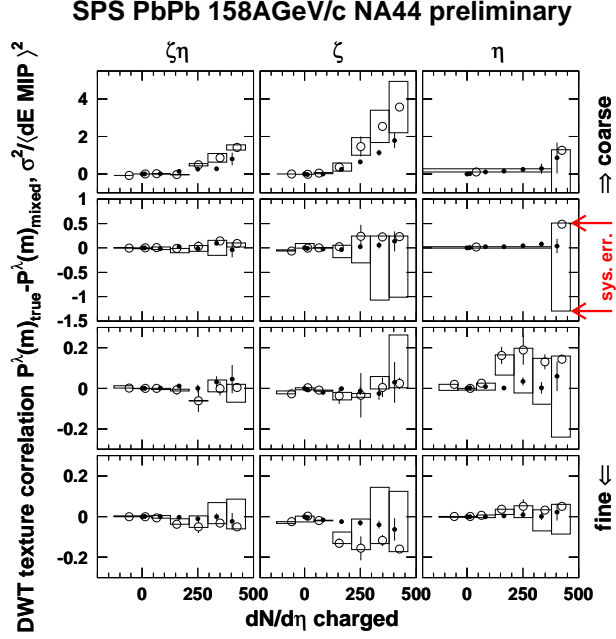


Figure 2. Multiplicity dependence of the texture correlation. \circ – the NA44 data, \bullet – RQMD. The boxes show the systematic errors vertically and the boundaries of the multiplicity bins horizontally; the statistical errors are indicated by the vertical bars on the points. The rows correspond to the scale fineness m , the columns – to the directional mode of the power spectrum λ (which can be diagonal $\zeta\eta$, azimuthal ζ , and pseudorapidity η).

constitute the subevents subjected to the event number scrambling. In other words, the mixed events preserve the texture coupled with the channels of the detector. This is *static* texture as it reproduces its pattern event after event; we are interested in *dynamic* texture. We reduce sources of static texture in the power spectra by empty target subtraction and by subtraction of the mixed events power spectra, thus obtaining the *texture correlation* $P^\lambda(m)_{true} - P^\lambda(m)_{mixed}$. Its multiplicity dependence is plotted on Figure 2. For comparison with models, a MC simulation (done with RQMD¹³) includes the known static texture effects and undergoes the same elimination procedure. This allows the effects irreducible by the subtraction methods to be taken into account in the comparison. One such example is the finite beam size, which has been shown by the MC studies to cause the RQMD points to rise with $dN/d\eta$.

The systematic errors were evaluated by removing the Pb target and switching magnetic field polarity to expose the analyzed side of the detector to δ -electrons, while minimizing nuclear interactions. All correlations (i.e. deviations of $P^\lambda(m)_{true}$ from $P^\lambda(m)_{mixed}$) in such events are considered to be systematic errors. Thus this component of the systematic error gets a sign, and the systematic errors are asymmetric. The other component (significant only on the coarsest scale) is the uncertainty of our knowledge of the beam's geometrical cross-section.

This novel method of event-by-event analysis, applied to the SPS $PbPb$ data, does not reveal any evidence of critical phenomena.

The authors thank N.Antoniou, I.Dremin, E.Shuryak, M.Stephanov, and T.Trainor for illuminating discussions. The NA44 Collaboration thanks the staff of the CERN PS-SPS accelerator complex for their excellent work, and the technical staff in the collaborating institutes for their valuable contributions. This work was supported by the Austrian Fonds zur Förderung der Wissenschaftlichen Forschung; the Science Research Council of Denmark; the Japanese Society for the Promotion of Science; the Ministry of Education, Science and Culture, Japan; the Science Research Council of Sweden; the US Department of Energy and the National Science Foundation.

References

1. N.M.Astafeva, I.M.Dremin, K.A.Kotelnikov, Mod. Phys. Lett. **A12** 1185-1192 (1997); I.M.Dremin et al, hep-ph/0007060.
2. NA49 Collaboration, Phys. Lett. **B459**, 679-686 (1999)
3. namely, by using the Central Limit Theorem – see: T.A.Trainor, hep-ph/0001148.
4. D.J.Scalapino, R.L.Sugar, Phys. Rev. **D8**, No 7, 2284-2294 (1973)
5. P.Carruthers, I.Sarcevic, Phys. Lett. **B189**, No 4, 442-448 (1987)
6. M.Stephanov, K.Rajagopal, E.Shuryak, Phys. Rev. Lett. **81** 4816 (1998)
7. I.Daubechies, Ten Lectures on Wavelets, SIAM, 1992
8. NA44 Collaboration, Phys. Lett. **B302** (1993) 510.
9. E. Beuville *et al.*, NIM **A288**, 157-167 (1990)
10. J.Pando, L-Z.Fang, Phys. Rev. **E57**, 3593-3601 (1998); L-Z.Fang, atroph/9791228.
11. N. Wiener, Generalized Harmonic Analysis.
12. G. Uytterhoeven *et al.*, WAILI: Wavelets with Integer Lifting. TW Report 262, Department of Computer Science, Katholieke Universiteit Leuven, Belgium, July 1997.
13. H. Sorge, Phys. Rev. C **52** (1995) 3291; we use version 2.4 of RQMD.